REFERENCES AND NOTES

1. P. J. Hagerman, *Annu. Rev. Biophys. Biophys. Chem.* **17**, 265 (1988).
2. M. Yanagida, Y. Hiraoka, I. Katsura, *Cold Spring Harbor Symp. Quant. Biol.* **47**, 177 (1983).
3. T. W. Houseal, C. Bustamante, R. F. Stump, M. F. Maestre, *Biophys. J.* **56**, 507 (1989).
4. S. B. Smith, P. K. Aldridge, J. B. Callis, *Science* **243**, 203 (1989).
5. D. C. Schwartz and M. Koval, *Nature* **338**, 520 (1989).
6. C. Bustamante, *Annu. Rev. Biophys. Biophys. Chem.* **20**, 415 (1991).
7. Single DNA molecule elasticity have been previously estimated by other authors (*2, 3*) using various ways of stretching, including optical tweezers [M. Kasevich *et al.*, *Proceedings of the Twelfth International Conference on Atomic Physics*, J. C. Zorn and R. R. Lewis, Eds. (American Institute of Physics, New York, 1990), pp. 53–57; S. Chu, *Science* **253**, 861 (1991)]. However, all of these methods measure the rate of contraction of a stretched molecule and require an estimation of the DNA drag coefficient. The static experiments presented here avoid this requirement.
8. B. H. Zimm and S. D. Levene, *Q. Rev. Biophys.*, in press.
9. B. Åkerman, M. Jonsson, B. Norden, *Biopolymers* **28**, 1541 (1989).
10. D. Stigter, *ibid.* **31**, 169 (1991).
11. F. Bueche, *Physical Properties of Polymers* (Interscience, New York, 1962), p. 37. No account is made in the derivation of Eq. 1 for the volume excluded from the polymer by the glass surface. However, although the presence of the wall reduces the number of accessible configurations to the chain [see E. F. Cassasa, *Polym. Lett.* **5**, 773 (1967); E. A. Di Marzio, *J. Chem. Phys.* **42**, 2101 (1965)], the tension in the chain, which is proportional to the gradient of its configurational entropy, is not affected in directions parallel to the plane of the wall, along which the chain is pulled.
12. P. J. Flory, *Statistical Mechanics of Chain Molecules* (Hanser, Munich, 1989), pp. 307–338 and 401.
13. Ligated 97-kbp dimers of methylated phage λ DNA, strain c1857ind1 Sam 7 (NEB) were used. The left sticky end of the dimer is hybridized and ligated to a 12-base oligo, 3′ end-labeled previously with digoxigenin (Boehringer Genius-5). The right sticky end is similarly attached to a 12-base oligo constructed with a 3′ biotin end-label (Glenn Research). The glass microscope slide is successively coated with γ-aminopropyltriethoxysilane (Pierce), protein A, polyclonal antidigoxigenin (Boehringer), and finally cross-linked with dimethyl pimelimidate (Pierce). The molecule ends were labeled differently to prevent attachment of both ends of the DNA to either the glass or the bead. The DNA is free to swivel about either point of attachment.
14. All equilibrium bead positions are time averages over the Brownian motion. Error is incurred when the position is averaged for a limited time with low-force points requiring longer times. For forces below 30 fN, averaging times >5 min yield errors of ±1 μm. High-force extensions can be measured in a few seconds to within ±0.3 μm.
15. C. R. Cantor and P. R. Schimmel, *Biophysical Chemistry Part II* (Freeman, New York, 1980), pp. 557–558.
16. The radius of a particular bead is checked through the optical microscope to within ±3%, leading to 3% uncertainty in the force, in addition to possible systematic error in the hydrodynamic radius. The viscous drag coefficient was checked by observing beads of known density fall through water. Equating the underwater weight with the Stokes' law drag gave a hydrodynamic radius 6% greater than the observed mechanical radius of 2.9 μm. This difference could be due to surface roughness or it could be an error in our estimate of the bead's volume due to porosities. The mechanical radius was used in all of the experiments shown here.
17. Close examination of Fig. 2A shows the molecules are curved because of hydrodynamic drag of DNA, which can be determined with only the curve shape and the bead radius, assuming a homogeneous flow field. The drag coefficient for a λ-dimer obtained is roughly one-half of that of a 2.9-μm bead. As a result, the tension next to the slide end of the molecule exceeds that at the bead end by as much as 50% in high flows. The tension that is measured by the angle method (caption to Fig. 1B) and plotted as force data is the average tension in the molecule. The curvature of DNA in Fig. 2A increases its path length only a negligible amount.
18. H. A. Lorentz, *Abhandlungen über Theoretische Physik* (Teubner, Leipzig, 1907), pp. 23–42.
19. Only one region of λ-DNA is highly bent, as shown by the anomalous gel mobility it confers to restriction fragments [see K. Zahn and F. R. Blattner, *Nature* **317**, 451 (1985)]. This region is unlikely to account for these results by itself, however, DNA curvature associated with random sequences could be both appreciable and ubiquitous (*21, 22*).
20. E. N. Trifonov, R. K.-Z. Tan, S. C. Harvey, in *Structure and Expression*, vol. 3: *DNA Bending and Curvature*, W. K. Olson, R. H. Sarma, M. Sundaralingam, Eds. (Adenine, New York, 1987), pp. 243–253.
21. A. Bolshoy, P. McNamara, R. E. Harrington, E. N. Trifonov, *Proc. Natl. Acad. Sci. U.S.A.* **88**, 2312 (1991).
22. Persistence length is a measure of the tendency of a chain to persist in some initial direction. Deflections from this direction can be caused by either thermal fluctuations or permanent bends. An inherently straight molecule at finite temperature would display a purely dynamic persistence length due to thermal fluctuations. An inherently bent molecule would display only its static persistence length at 0 K and an apparent persistence length at finite temperature.
23. P. J. Hagerman, *Biopolymers* **20**, 1503 (1981); E. S. Sobel and J. A. Harpst, *ibid.* **31**, 1559 (1991).
24. H. J. Vollenweider, A. James, W. Szybalski, *Biochemistry* **75**, 710 (1978).
25. The ethidium insensitivity of the "corner cutting" in the force curves is somewhat surprising. We can only list here the possible explanations: (i) ethidium does not bind to the bent regions in DNA; (ii) ethidium binds to bent regions but it does not change the local curvature; (iii) ethidium undoes the curvature of the bent regions but induces new curvature in inherently straight locations leading to a compensation effect; and (iv) corner cutting is not caused by bent regions. The latter is less likely as shown by the DDP experiments further in the text.
26. W. D. Wilson *et al.*, *Biochemistry* **29**, 8452 (1990).
27. G. Manzini, M. L. Barcellona, M. Avitabile, F. Quadrifoglio, *Nucleic Acids Res.* **11**, 8861 (1983).
28. N. P. Johnson *et al.*, in *Progress in Clinical Biochemistry and Medicine* (Springer-Verlag, Berlin, 1989), vol. 10, pp. 1–24.
29. J.-P. Macquet and J.-L. Butour, *Biochemie* **60**, 901 (1978).
30. W. Saenger, *Principles of Nucleic Acid Structure* (Springer-Verlag, New York, 1984), p. 226.

31. We thank J. Schellman, H. Reese, N. Johnson, and P. Sebring for many useful discussions. Supported by National Institutes of Health grant GM 32543 and National Science Foundation MCB 9118482 to C.B. Additional Funding was provided by the Lucille P. Markey Charitable Trust.

17 July 1992; accepted 10 September 1992

Complete Wetting from Polymer Mixtures

Ullrich Steiner, Jacob Klein,* Erika Eiser, Andrzej Budkowski,† Lewis J. Fetters

Coexisting polymer phases are characterized by very small interfacial energies, even well below their critical solution temperature. This situation should readily lead to the exclusion of one of the phases from any interface that favors the other. Such complete wetting behavior from a binary mixture of statistical olefinic copolymers is reported. By means of a self-regulating geometry, it is found that the thickness of a wetting layer of one of the phases at the polymer-air interface, growing from the other coexisting phase, attains macroscopic dimensions, increasing logarithmically with time. These results indicate that binary polymer mixtures could be attractive models for the study of wetting phenomena.

A surface in contact with a mixture of two fluid phases will generally favor one of them. The surface may be partially wetted, in which case it will be covered by a microscopic layer of the favored phase, or it may be covered by a thick, macroscopic layer of this phase for the case of complete wetting (*1*). This transition between partial and complete wetting is implicit in the early work of Young (and of Laplace) on the contact angle of liquid drops on a surface (*2*), but it is only recently that the physics of such transitions has come into sharper focus. In a seminal paper (*3*), Cahn in 1977 proposed that a transition from partial to complete wetting from a binary mixture must always occur when the temperature T is raised sufficiently close to the upper critical solution temperature T_c (the highest temperature at which two phases can coexist) of the mixture. In the ensuing years, there have been extensive theoretical and experimental studies of such transitions (*4, 5*). Among the outstanding unresolved issues is that of wetting from macromolecular mixtures (*6, 7*). In these mixtures, complete wetting is predicted to occur readily, and far from T_c (*7*); yet such wetting has

U. Steiner, J. Klein, E. Eiser, A. Budkowski, Department of Materials and Interfaces, Weizmann Institute of Science, Rehovot 76100, Israel.
L. J. Fetters, Exxon Research and Engineering Corporation, Annandale, NJ 08801.

*To whom correspondence should be addressed.
†On leave from Jagellonian University, Cracow, Poland.

never been observed (*8*). Here we demonstrate unambiguously that complete wetting occurs from a binary polymer mixture. Using a self-regulating geometry, we were able to follow in detail the growth of the wetting layer from such a mixture near its phase-coexistence boundary. Our results suggest that polymeric blends may provide attractive models for the study of wetting from binary mixtures.

Wetting of a surface of phase C from a mixture of A and B is determined by the relation

$$\gamma_{c\beta} - \gamma_{c\alpha} \leq \gamma_{\alpha\beta} \quad (1)$$

Here α and β are the coexisting A- and B-rich phases, respectively; the surface of C has a preference for the α phase, and γ_{xy} is the interfacial energy between the x and y phases: inequality in relation 1 implies that at equilibrium surface C is only partially wetted, whereas at equality the surface will be completely wetted (*9*).

In mixtures of small molecules, the interaction parameters governing the values of the interfacial energies, and therefore of both sides of relation 1, are frequently comparable (*1*). Cahn proposed (*3*) that, near T_c, the interfacial energy $\gamma_{\alpha\beta}$ between the coexisting α and β phases must decrease more rapidly with $(T_c - T)$ than does the difference $(\gamma_{c\beta} - \gamma_{c\alpha})$ (*10*). In consequence, sufficiently close to T_c, any inequality in relation 1 corresponding to partial wetting will always become an equality, that is, complete wetting.

This argument, although compelling, is not always valid: later researchers showed (*4*) that the argument could be violated if there were competing short- and long-range interactions at the surface-fluid interface. Nonetheless, for most binary mixtures studied, complete wetting does occur over a finite temperature range between T_c and a wetting transition temperature T_w (*4*). For polymer mixtures the situation is qualitatively different. The monomer-surface interactions, and the values of $\gamma_{c\beta}$ and $\gamma_{c\alpha}$ and of the left side of relation 1, remain comparable to those of their small-molecule analogs; but there is a massive reduction (by a factor N, the number of monomers per chain) in the entropic factors promoting mixing between the different polymers (*11*). This reduction gives rise to a monomer-monomer interaction parameter χ_c at T_c that is extremely small (of order $1/N$), and implies interfacial energies $\gamma_{\alpha\beta}$ that are very weak even far below T_c.

Thus, for polymer mixtures, equality in relation 1 and a transition to complete wetting should occur readily at $T_w << T_c$. This transition must take place on the phase-coexistence line, and the above considerations suggest that it occurs at a very low volume fraction ϕ^A_w of the surface-preferred A component (*7*). In order to observe complete wetting, it is then necessary that the polymer phase adjacent to the wetted surface be on the coexistence line, and at a volume fraction $\phi^A \geq \phi^A_w$. In our experiments we have ensured precisely this situation, as illustrated schematically in Fig. 1.

The polymers used are statistical copolymers (that is, the two monomer types are randomly distributed along the polymer chains) of ethylene and ethyl-ethylene monomers, $(C_4H_8)_x$-$[C_2H_3$-$(C_2H_5)]_{1-x}$,

Table 1. Molecular characteristics of statistical copolymers with monomer structure $(C_4H_8)_x$-$[C_2H_3(C_2H_5)]_{1-x}$, where x is the relative vinyl content of the PBD precursor polymer; the weight- and number-averaged molar masses, M_w and M_n, were determined by light scattering and size exclusion chromatography, respectively; their ratio is a measure of the sample polydispersity. The level of deuteration was determined by density measurements (*12*); T_g is the glass transition temperature.

Polymer	x	N	M_w/M_n	^2H per monomer	T_g (°C)
dC	0.12	1610	1.03	2.96	−34
hE	0.22	1290	1.02		−45

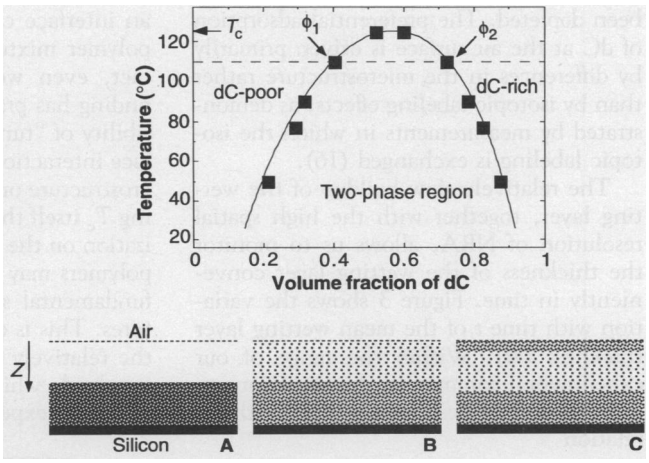

Fig. 1. The geometry used to observe wetting in our study. (**A**) Initially a layer (~350 nm thick) of pure dC is spin-cast on a polished silicon wafer, and a similar layer of pure hE is mounted on top to form a bilayer separated by a sharp interface. (**B**) On annealing at T_1(110°C) < T_c the polymers interdiffuse, and bulk transport takes place across the interface, driving the compositions in the layers toward their coexisting values ϕ_1 (dC-poor, lightly shaded) and ϕ_2 (dC-rich, heavier shading). (**C**) The polymer-air interface interacts preferentially with the dC molecules to form a dC-rich phase (composition ϕ_2) at the air surface, growing from the dC-poor phase. The ϕ_2 phase at the silicon surface acts as the (progressively shrinking) reservoir for the wetting layer. The composition profile with depth z of the partly deuterated dC component was determined by NRA (*14*). The inset shows the phase-coexistence curve for the dC-hE mixture. We determined this curve (*15*) by reversing the order of the layers on the surface, letting them interdiffuse to coexistence at different temperatures, and measuring the coexisting compositions (by NRA) for each temperature. The horizontal line shows the temperature of the present wetting experiments.

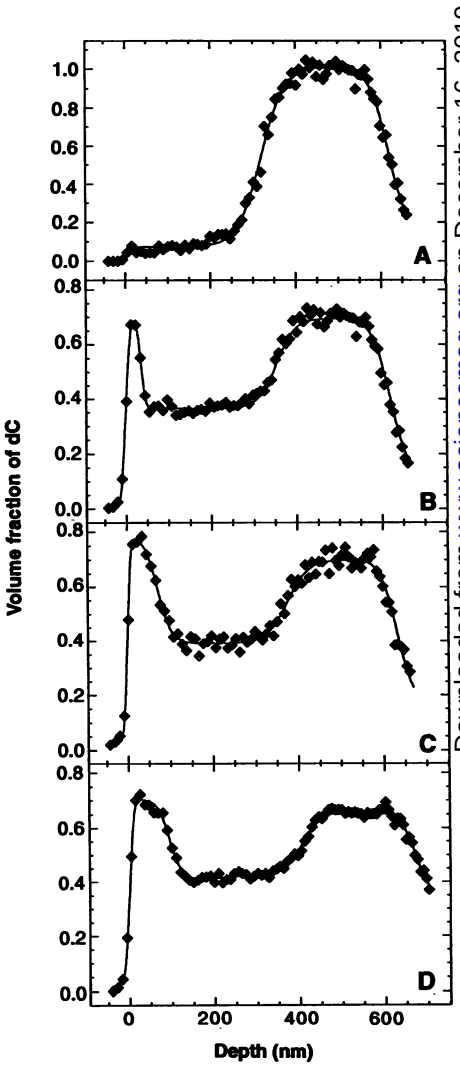

Fig. 2. Composition-depth profile of the dC molecules in the bilayer after increasing annealing times t at 110°C. Zero depth corresponds to the air surface, with the silicon surface at ~650 nm: (**A**) unannealed; (**B**) t = 30 min; (**C**) t = 8.0 hours; (**D**) t = 3.0 days. The compositions of the dC-rich phase near the silicon surface and of the dC-poor phase adjacent to it correspond to ϕ_2 and ϕ_1, respectively (inset to Fig. 1).

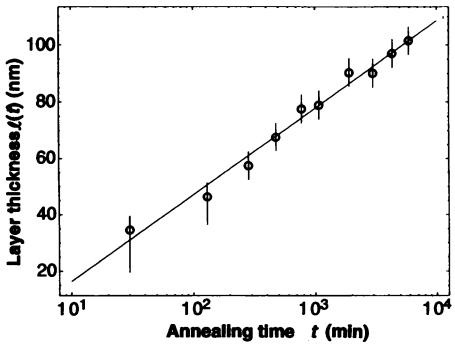

Fig. 3. Variation with time of the mean thickness of the dC-rich wetting layer at the air interface.

made by anionic polymerization of polybutadiene (PBD) followed by hydrogenation [or deuteration, where ^2H labeling is required (*12*)]. Their composition (that is, x) is controlled by the vinyl content of the PBD precursor, and one can "tune" the interaction of such random copolymers with each other (*12*) and with surfaces by varying x. The molecular characteristics of the pair used in the present study, designated dC and hE, are given in Table 1. Samples were prepared by spin coating a film (approximately 350 nm thick) of dC from toluene onto a polished silicon wafer; a similar film of hE was mounted on top of dC to form a bilayer [as illustrated in Fig. 1A (*13*)]. The bilayers were placed in a vacuum oven (10^{-2} torr) at a temperature T_1 of 110° ± 0.5°C, and the composition profile normal to the polymer-air surface within each sample was determined by nuclear reaction analysis [NRA (*14*)] for different annealing times t. In separate experiments the phase-coexistence curve of the binary hE-dC pair was determined [by NRA (*15*)] and is reproduced in the inset to Fig. 1. The coexistence curve indicates that for this system T_c = 126° ± 2°C.

Figure 2 shows the composition-depth profiles of the polymer bilayers normal to the sample surface after increasing annealing times. The initially sharp interface of the unannealed sample (Fig. 2A) broadens by interdiffusion upon annealing. After 30 min (Fig. 2B) the plateau composition levels of the two phases, which change as a result of bulk transport, are close to their coexisting values (inset in Fig. 1); at the same time a clear surface peak of the dC-rich phase is observed. The width $\ell(t)$ of this peak increases over the entire range of annealing times t, as shown in Fig. 2, B to D. This width at times longer than a few hours is much larger than the spatial resolution [about 10 nm (*14*)] of the NRA depth profiling technique and is also larger than any microscopic correlation lengths in the mixture, such as the equilibrium width of the interface separating the coexisting phases (*14*). The data thus show clearly the growth with time of a macroscopic dC-rich layer at the sample-air interface. The composition of this layer is the same, within the scatter, as that of the dC-rich phase adjacent to the silicon substrate, whereas the plateau composition of the intervening layer is that of the coexisting dC-poor phase (Fig. 2).

These observations are direct and readily interpreted. Annealing of the bilayer at a temperature $T_1 < T_c$ leads to bulk transport across the interface separating the initially pure dC and hE layers. In the absence of any preferential surface interactions, one expects a dC-poor phase (phase composition ϕ_1) adjacent to the air surface to coexist at equilibrium with a dC-rich phase (ϕ_2) adjacent to the silicon. In our system there is a preferential attraction for the dC component at the polymer-air interface: thus, as the dC concentration adjacent to this interface increases, a dC-rich surface layer begins to form. As the composition of the near-surface region evolved toward ϕ_1 (Figs. 1B and 2B), this layer increased from microscopic dimensions to a macroscopic surface phase of composition ϕ_2 (Figs. 1C and 2, C and D). The geometry of the system is self-regulating in that the near-surface phase from which the surface layer is growing always has a composition close to ϕ_1 and coexists with the progressively shrinking reservoir of the ϕ_2 phase on the silicon surface.

This result unambiguously shows complete wetting of the polymer-air surface by the dC-rich phase from the coexisting dC-poor phase. Although a thickening of the wetting layer up to ~100 nm is documented here, its growth stops only when all the ϕ_2 phase initially on the silicon surface has been depleted. The preferential adsorption of dC at the air surface is driven primarily by differences in the microstructure rather than by isotopic labeling effects, as demonstrated by measurements in which the isotopic labeling is exchanged (*16*).

The relatively slow buildup of the wetting layer, together with the high spatial resolution of NRA, allows us to monitor the thickness of the wetting layer conveniently in time. Figure 3 shows the variation with time t of the mean wetting layer thickness $\ell(t)$. Within the range of our experimental parameters, this variation appears to be best described by a logarithmic relation

$$\ell(t) \sim \log(t) \qquad (2)$$

as shown by the line in Fig. 3 (*17*).

To our knowledge, there have been no comparable experimental kinetic studies of mixtures of small-molecule fluids. In such systems convectional flows between surface and bulk, as well as gravitational potentials, can complicate the interpretation of the dynamic behavior (*18*, *19*); in addition, initial wetting may occur through the growth of droplets of the wetting phase on the surface (*4*, *5*). In our polymeric mixture the chains are highly entangled, so that any convectional flow is likely to be strongly suppressed, and the wetting layer grows primarily by diffusional processes. Moreover, in the forward-scattering configuration of the NRA used for the compositional profiling in our experiments, the presence of discrete dC-rich droplets would be readily detected as an anomalous systematic broadening of the interface between the wetting layer and the dC-poor phase adjacent to it (*14*). Careful checks revealed no such broadening, from which we conclude that the wetting layer is growing uniformly inward from the polymer-air interface into the polymer bulk. There are few calculations of the thickening kinetics of wetting layers from binary mixtures with which we may compare our results (*20*, *21*). For the case of long-range intermolecular forces and diffusion-limited growth, the likely situation with our nonpolar polymer molecules, a weak power law is predicted (*21*) for the increase of $\ell(t)$ with time; but the theoretical situation is far from resolved (*4*).

We come finally to the question of the wetting transition in polymer mixtures. Complete wetting from the dC-hE system documented here occurred at 16°C below T_c; in similar experiments with a binary mixture of analogous copolymers (but with different x values) we observed complete wetting of the air interface even at some 100°C below the respective T_c, from a coexisting phase containing only some 10% of the surface-preferred component (*22*).

Our results demonstrate that wetting of an interface can take place readily from a polymer mixture with which it is in contact, even well away from its T_c. This finding has practical implications; the possibility of "tuning" intermolecular and surface interactions through the monomer microstructure on the one hand and of adjusting T_c itself through the degree of polymerization on the other hand suggests also that polymers may be good model materials for fundamental studies of wetting from mixtures. This is especially the case in view of the relatively large spatial and time scales involved, which can be conveniently accessed by experiment.

REFERENCES AND NOTES

1. J. S. Rowlinson and B. Widom, *Molecular Theory of Capillarity* (Clarendon, Oxford, 1982).
2. T. Young, *Philos. Trans. R. Soc. London* **95**, 65 (1805).
3. J. W. Cahn, *J. Chem. Phys.* **66**, 3667 (1977).
4. P. G. de Gennes, *Rev. Mod. Phys.* **57**, 827 (1985); S. Dietrich, in *Phase Transitions and Critical Phenomena*, C. Domb and J. Lebowitz, Eds. (Aca-

demic Press, London, 1988), vol. 12, pp. 1–218; M. Schick, in *Liquids at Interfaces*, Les Houches session XLVIII, 1988, J. Charvolin, J.-F. Joanny, J. Zinn-Justin, Eds. (Elsevier, Amsterdam, 1990), pp. 419–497; D. Beysens, *ibid.*, pp. 502–548.
5. D. J. Durian and C. Franck, *Phys. Rev. A* **40**, 5220 (1989).
6. H. Nakanishi and P. Pincus, *J. Chem. Phys.* **79**, 997 (1983).
7. I. Schmidt and K. Binder, *J. Phys. (Paris)* **46**, 1631 (1985).
8. Surface enrichment by one of the components from a binary polymer mixture, extending to a bulk correlation length away from the surface, has been observed in polystyrene(PS)/poly(vinyl methylether) blends by Q. S. Bhatia, D. H. Pan, and J. T. Koberstein [*Macromolecules* **21**, 2166 (1988)] and by R. A. L. Jones *et al.* [*Phys. Rev. Lett.* **62**, 280 (1989)] for the case of deuterated PS/protonated PS mixtures. This corresponds to partial wetting.
9. This condition is fully equivalent to the disappearance of the dihedral angle θ between contacting phases in the classical Young-Dupre equation $\gamma_{c\beta} = \gamma_{c\alpha} + \gamma_{\alpha\beta} \cos\theta$. A clear discussion of this is given by Schick [in (*4*)].
10. This is so because $(\gamma_{c\beta} - \gamma_{c\alpha})$ is proportional to the difference between the densities of the α and β phases (or, in the case of binary mixtures, to the difference between their compositions), and this difference is known from experiment (*4*) to decrease to zero more slowly with $(T_c - T)$ than does $\gamma_{\alpha\beta}$.
11. P. J. Flory, *Principles of Polymer Chemistry* (Cornell Univ. Press, Ithaca, NY, 1953); P. G. de Gennes, *Scaling Concepts in Polymer Physics* (Cornell Univ. Press, Ithaca, NY, 1975).
12. N. P. Balsara *et al.*, *Macromolecules*, in press.
13. It is essential, when floating spin-cast films of these rubbery polymers on water to create the bilayers, that contact with the water be minimized. Details of the procedure are to be published (*15*).
14. In this technique a beam of ^{3}He particles is incident on the thin, partially deuterated polymer sample, and energetic α-particles [^{4}He] from the reaction

$$^3\text{He} + {}^2\text{H} \rightarrow {}^4\text{He} + {}^1\text{H} + 18.352\ \text{MeV}$$

are detected at a forward angle. From the energy spectrum of the α-particles, known energy losses within the sample, and the reaction cross section, composition-depth profiles of the deuterium-labeled chains are directly obtained. Details are given in the following: U. K. Chaturvedi, U. Steiner, G. Krausch, G. Schatz, J. Klein, *Phys. Rev. Lett.* **63**, 616 (1989); *Appl. Phys. Lett.* **56**, 1228 (1990); J. Klein, *Science* **250**, 640 (1990); (*15*).
15. E. Eiser, A. Budkowski, U. Steiner, J. Klein, L. J. Fetters, in preparation. See also A. Budkowski, U. Steiner, J. Klein, G. Schatz, *Europhys. Lett.* **18**, 705 (1992).
16. In contrast to the polymer-air interface which is wetted by the dC-rich phase, we saw no wetting by either phase at the polymer-silicon interface. After very long annealing times, we observed nucleation and the growth of holes in the polymer layer.
17. There appears to be a systematic deviation of the data from a straight line on a plot of $\log[\ell(t)]$ versus $\log(t)$, but a weak power-law type behavior, $\ell(t) \sim t^{\theta}$, cannot be entirely ruled out.
18. R. F. Kayser, J. W. Schmidt, M. R. Moldover, *J. Chem. Soc. Faraday Trans. 2* **82**, 1701 (1986).
19. P. Guenoun, D. Beysens, M. Robert, *Phys. Rev. Lett.* **65**, 2406 (1990).
20. R. Lipowsky, *J. Phys. A: Gen. Phys.* **18**, L585 (1985); K. Binder, in *Kinetics of Ordering and Growth at Surfaces*, M. G. Lagally, Ed. (Plenum, New York, 1990), p. 31, and references therein.
21. R. Lipowsky and D. A. Huse, *Phys. Rev. Lett.* **52**, 353 (1986).
22. We are currently extending our experiments to probe the question of where the partial-to-complete wetting transition occurs, and its order in polymer mixtures, as well as to characterize explicitly the surface interaction parameters that are involved. Partial wetting in the configuration of our experiments would result in wetting layers of finite thickness (comparable with bulk correlation lengths) in equilibrium, as in the studies (*8*) showing surface enrichment from a one-phase polymer mixture.
23. We thank K. Binder, P. Pincus, and S. Safran for fruitful discussions and critical reading of the manuscript. This work was supported by the German-Israel Foundation, the U.S.–Israel Binational Science Foundation, and the Minerva Foundation. J.K. is the incumbent of the Herman Mark Chair in Polymer Physics at the Weizmann Institute.

24 June 1992; accepted 3 September 1992

Electron Photodetachment Cross Sections of Small Carbon Clusters: Evidence for Nonlinear Isomers

D. Zajfman, H. Feldman, O. Heber, D. Kella, D. Majer, Z. Vager, R. Naaman

Absolute cross sections for photodetachment of negative carbon clusters are reported for C_n^- (n = 3, . . ., 8). The results indicate that various neutral isomers exist, some with electron affinities as low as 1 electron volt. The method of production plays an important role in the characteristics of carbon clusters.

Pure carbon molecules are currently under intense experimental and theoretical scrutiny. These molecules are believed to play an important role in the formation of soot in flames and have been detected in interstellar space, being produced in giant carbon stars.

A review of the large amount of research that has been devoted to these molecules has been given by Weltner and van Zee (*1*). Until recently, the question of the molecular structure of such species was mainly addressed theoretically. The first theoretical calculation (*2*) suggested that carbon clusters of n atoms were either linear ($n \leq 10$) or rings ($n > 10$). Several recent high-level calculations (*3*) predict that planar monocyclic isomers exist for small even-numbered clusters (n = 4, 6, and 8). Experiments were not able to confirm this prediction, and only linear species were reported to have been detected (*4–6*). A sharp even-odd alternation in the electronic structure and stability was found: the even-numbered clusters are open-shell species with $^3\Sigma_g^-$ ground states and high electron affinities, whereas the odd clusters are closed-shell species with $^1\Sigma_g^+$ ground states and lower electron affinities. However, in recent photoelectron detachment studies there were indications that nonlinear isomers may exist (*6*). Also, indications for the existence of both linear and nonlinear isomers of C_7^+ to C_{10}^+ were reported recently (*7*).

In a previous experiment, we reported the observation of a cyclic C_4 (*8, 9*) using the Coulomb explosion imaging (CEI) technique (*10*) combined with laser photodetachment. We have extended these measurements to other clusters ($3 \leq n \leq 8$). We have measured the absolute photodetachment cross section of these clusters as a function of photon wavelength.

Figure 1 illustrates schematically the experimental arrangement. Negative ions were produced in either the standard Hiconex 834 cesium-beam sputter source or by a laser vaporization–pulsed molecular beam source. In the latter, a carrier gas could be introduced from a pulsed nozzle operating at a backing pressure of several atmospheres, which allowed relaxation of molecular degrees of freedom by collisions with the gas atoms as well as creation of larger clusters. After acceleration to an energy of ~100 keV, the negative ions were collimated by an aperture (2-mm diameter). A laser beam was directed colinearly with the ion beam and in the opposite direction. Either a Nd:Yag (fundamental, second, and third harmonic) or an excimer pumped dye laser was used in this experiment. The lasers operated at 25 Hz and were synchronized with an electrostatic chopper placed at the exit of the ion source, pulsing the negative ion beam into 20-μs-long pulses. The negative ions surviving the laser interaction were mass analyzed by a 90° magnet and detected by a microchannel plate (MCP). The laser intensity was measured by introducing a prism that deflected the light through a window to a power meter (Fig. 1).

The depletion of the negative ions due to the interaction with the laser photons was monitored by digital recording of the ion current (amplified by the MCP electron multiplier) as a function of time. A typical depletion curve as a function of time is shown in Fig. 2. The time resolution was chosen to be 0.25 μs, which is equivalent to a typical ion flight path of 10 cm. For a

D. Zajfman, H. Feldman, O. Heber, D. Kella, D. Majer, Z. Vager, Department of Nuclear Physics, Weizmann Institute of Science, Rehovot 76100, Israel.
R. Naaman, Department of Chemical Physics, Weizmann Institute of Science, Rehovot 76100, Israel.